



Role of fractionation correction in accurate determination of $^{142}\text{Nd}/^{144}\text{Nd}$ by TIMS: A case study of 1.48 Ga alkaline rocks from Khariar, India



Ikshu Gautam^{a,b,*}, Jyotiranjan S. Ray^a, Rajneesh Bhutani^c, S. Balakrishnan^c, J.K. Dash^c

^a Physical Research Laboratory, Ahmedabad 380 009, India

^b Department of Geology, The Maharaja Sayaji Rao University of Baroda, Vadodara 390002, India

^c Department of Earth Sciences, Pondicherry University, Puducherry 605 014, India

ARTICLE INFO

Keywords:

$^{142}\text{Nd}/^{144}\text{Nd}$ analyses
TIMS
1.48 Ga Khariar rocks

ABSTRACT

The short-lived isotopic systematics of ^{146}Sm - ^{142}Nd is a tracer of early silicate Earth differentiation events. Evidence for these events comes from anomalous $^{142}\text{Nd}/^{144}\text{Nd}$, defined in terms of $\mu^{142}\text{Nd}$ ($\mu^{142}\text{Nd} = \{[(^{142}\text{Nd}/^{144}\text{Nd})_{\text{sample}} / (^{142}\text{Nd}/^{144}\text{Nd})_{\text{standard}}] - 1\} \times 10^6$) with respect to a terrestrial standard representing the modern accessible mantle. This requires measurement of accurate and highly precise $^{142}\text{Nd}/^{144}\text{Nd}$, which is carried out by Thermal Ionisation Mass Spectrometry (TIMS). Since multiple factors affect the accuracy of the final results, we carried out a detailed investigation on the effect of various data acquisition, fractionation correction and normalization methods on the accuracy of $^{142}\text{Nd}/^{144}\text{Nd}$ determinations. Based on the analyses of Ames Nd standard using various combinations of the most commonly employed methods we observed that for a multi-dynamic mode of data acquisition, the *power-normalised exponential law* is the most appropriate method for mass fractionation correction. The time delays between successive sequences in a multi-dynamic mode had little effect on the final value of $^{142}\text{Nd}/^{144}\text{Nd}$. The different standards have different $^{142}\text{Nd}/^{144}\text{Nd}$ ratios and therefore, their uses yield different $\mu^{142}\text{Nd}$ values for the same sample. We extended this information to understand the two contradicting results from 1.48 Ga alkaline rocks from Khariar, India, carried out on the same sample aliquots (Upadhyay et al. 2009; Roth et al. 2014b). A confirmation of ^{142}Nd anomalies in such younger rocks is important because it could establish the longevity of early silicate differentiation signatures beyond Archean. Our experiment on freshly collected samples from the same outcrops, using identical analytical procedures, could not reproduce the results of Upadhyay et al. (2009). We did, however, observe slightly negative $\mu^{142}\text{Nd}$ values with respect to Ames Nd, which became normal with respect to JNdi-1.

1. Introduction

The near absence of rock record from the first 500 million years of the Earth's history makes it difficult to understand the earliest differentiation processes that caused the separation of its various reservoirs. Short lived radionuclides and their decay products have been useful in such studies as they provide critical information about these processes from meteorites and ancient magmatic systems. ^{146}Sm - ^{142}Nd ($t_{1/2} = 103$ Ma; (Marks et al., 2014) or 68 Ma; Kinoshita et al., 2012) is one such systematics which has been widely utilized to decode the early silicate Earth differentiation. Anomalous abundances of ^{142}Nd with respect to terrestrial standards, expressed as $\mu^{142}\text{Nd}$ ($\mu^{142}\text{Nd} = \{[(^{142}\text{Nd}/^{144}\text{Nd})_{\text{sample}} / (^{142}\text{Nd}/^{144}\text{Nd})_{\text{standard}}] - 1\} \times 10^6$), provide clues to fractionation of Sm/Nd during the differentiation events that took place during the first 500 million years of the Earth's formation, when ^{146}Sm was extant. Considering the highly dynamic nature of the

Earth's earliest mantle and the time elapsed since its formation, it is extremely difficult to encounter $\mu^{142}\text{Nd}$ anomalies in rocks younger than Archean. Also, because of the small magnitude of these anomalies and isobaric interferences of Sm and Ce on various Nd isotopes including ^{142}Ce (11.4% abundance) on ^{142}Nd (27.2%), their detection through mass spectrometry is analytically challenging. All of the accepted discoveries of $\mu^{142}\text{Nd}$ anomalies come from the Hadean and Archean rocks. The positive anomalies possibly represent the earliest Large Ion Lithophile Element (LILE) depleted source (Bennett et al., 2007; Boyet and Carlson, 2006; Boyet et al., 2003; Caro et al., 2006, 2003; Rizo et al., 2011). Only four examples of negative $\mu^{142}\text{Nd}$ anomalies are known today (O'Neil et al., 2008; Rizo et al., 2012; Roth et al., 2014a; Roth et al., 2013; Upadhyay et al., 2009), which are believed to be vestiges of a Hadean LILE enriched reservoir, possibly representing the earliest crust (Rizo et al., 2012; Roth et al., 2014a) and/or non-convecting lithospheric mantle (Upadhyay et al., 2009).

* Corresponding author.

E-mail address: ikshu@prl.res.in (I. Gautam).

Table 1

Comparison of various data acquisition and reduction procedures followed by Upadhyay et al. (2009) and Roth et al. (2014b).

Parameter	Upadhyay et al. (2009)	Roth et al. (2014b)
Number of sequences in multi-dynamic mode	Three	Two
Fractionation correction law	Power-law normalized exponential law	Exponential law
Fractionation factor	Average of all sequences : ($\beta_1 + \beta_2 + \beta_3$)/3	Calculated from sequence 1: β_1
Cup factors	Get cancelled	Do not get cancelled ^a
Multi-dynamic correction for ratios	$^{142}\text{Nd}/^{144}\text{Nd}$, $^{143}\text{Nd}/^{144}\text{Nd}$, $^{145}\text{Nd}/^{144}\text{Nd}$, $^{148}\text{Nd}/^{144}\text{Nd}$	$^{142}\text{Nd}/^{144}\text{Nd}$
Static correction for ratios	$^{150}\text{Nd}/^{144}\text{Nd}$	$^{143}\text{Nd}/^{144}\text{Nd}$, $^{145}\text{Nd}/^{144}\text{Nd}$, $^{148}\text{Nd}/^{144}\text{Nd}$, $^{150}\text{Nd}/^{144}\text{Nd}$

^a As described in Roth et al. (2014b), the cup factors do not affect the exponential law corrected $^{142}\text{Nd}/^{144}\text{Nd}$ by > 5 ppm if the difference in relative cup efficiency is < 370 ppm. The relative cup efficiency is calculated by taking the difference of static $^{142}\text{Nd}/^{144}\text{Nd}$ measured in sequence 1 and 2.

Significantly, one of these negative anomalies was reported from 1.48 Ga alkaline rocks by Upadhyay et al. (2009), a finding that has the potential to change our understanding of the preservation and longevity of the evidence for the earliest crust-mantle differentiation. Since these rocks are believed to have originated from the lithospheric mantle, the authors argued for preservation of ^{142}Nd anomaly in a non-convective mantle domain in cratonic roots for at least for 2.7 billion years since its formation (Upadhyay et al., 2009, 2006). However, if these anomalies turn out to be analytical artefact then the hypothesis of continental lithospheres being sites of preservation of ^{142}Nd anomalies would be invalidated, restricting the anomalous signals only to the rocks of Hadean and Archean. Therefore, it is imperative that the robustness of these results is verified through independent investigations by different laboratories.

In an attempt to verify the negative ^{142}Nd anomalies in the 1.48 Ga Khariar samples, Roth et al. (2014b) measured $^{142}\text{Nd}/^{144}\text{Nd}$ in the same aliquots of the samples of Upadhyay et al. (2009), but could not reproduce the results. In their data acquisition protocol on TIMS, Roth et al. (2014b) had employed a 2-sequence multi-dynamic mode in contrast to a 3-sequence mode utilized by Upadhyay et al. (2009). To

minimize the time delay between the measurements of $^{144}\text{Nd}/^{146}\text{Nd}$ and $^{142}\text{Nd}/^{144}\text{Nd}$, Roth et al. (2014b) acquired these ratios in sequences 1 and 2, instead of sequences 1 and 3 as followed by Upadhyay et al. (2009). This was done to remove the analytical bias in the (mass) fractionation corrected $^{142}\text{Nd}/^{144}\text{Nd}$ in the 3-sequence mode, caused by higher relative rate of fractionation ($r_f > 1$). Where r_f = average fractionation rate (r_a) / threshold fractionation rate (r_t), and r_t = external reproducibility / time gap between the sequences (1 and 2 in 2-sequence mode or 1 and 3 in 3-sequence mode). Average fractionation rate is calculated for each analysis by finding the slope of the regressed line when uncorrected $^{146}\text{Nd}/^{144}\text{Nd}$ from sequence-1 is plotted against the time.

Roth et al. (2014b) also proposed a correction procedure to reduce the 3-sequence data of Upadhyay et al. (2009), where r_t was lower than that in a 2-sequence mode, and showed that in all except one sample the anomalies vanished. According to the authors, this correction procedure was not advocated for general use, but rather is an approximation to re-assess published data. The number of sequences was not the only analytical parameter that was different in the two studies. Another important parameter which was not given a due importance was the

Table 2

Details of fractionation correction methods used in the present study. When exponential law is used to correct data acquired using 3-sequence multi-dynamic mode, sequence 2 in the given formulae are replaced by sequence 3.

Isotopic ratio	Power - normalised exponential law	Exponential law
$^{142}\text{Nd}/^{144}\text{Nd}$	$[(^{142}\text{Nd}/^{144}\text{Nd})_3 \times (^{146}\text{Nd}/^{144}\text{Nd})_1 / 0.7219] \times (141.907731/143.910096)^\beta \times (1 + f)^2$	$[(^{142}\text{Nd}/^{144}\text{Nd})_2] \times (141.907731/143.910096)^\beta$
$^{143}\text{Nd}/^{144}\text{Nd}$	$\{[(^{143}\text{Nd}/^{144}\text{Nd})_2 \times (^{143}\text{Nd}/^{144}\text{Nd})_3] / [(^{144}\text{Nd}/^{146}\text{Nd})_1 \times 0.7219]\}^{0.5} \times (142.909823/143.910096)^\beta \times (1 + f)^1$	$[(^{143}\text{Nd}/^{144}\text{Nd})_1] \times (142.909823/143.910096)^\beta$
$^{145}\text{Nd}/^{144}\text{Nd}$	$\{[(^{145}\text{Nd}/^{144}\text{Nd})_2 \times (^{145}\text{Nd}/^{146}\text{Nd})_1 \times 0.7219]\}^{0.5} \times (144.912582 / 143.910096)^\beta \times (1 + f)^{-1}$	$[(^{145}\text{Nd}/^{144}\text{Nd})_1] \times (144.912582 / 143.910096)^\beta$
$^{148}\text{Nd}/^{144}\text{Nd}$	$\{[(^{148}\text{Nd}/^{146}\text{Nd})_1 \times (^{144}\text{Nd}/^{146}\text{Nd})_3 \times (0.7219)^2]\} \times (147.916901 / 143.910096)^\beta \times (1 + f)^{-4}$	$[(^{148}\text{Nd}/^{144}\text{Nd})_1] \times (147.916901/143.910096)^\beta$
$^{150}\text{Nd}/^{144}\text{Nd}$	$[(^{150}\text{Nd}/^{144}\text{Nd})_1] \times (149.9209/143.910096)^\beta$	$[(^{150}\text{Nd}/^{144}\text{Nd})_1] \times (149.9209/143.910096)^\beta$

Here $\beta = \frac{(\beta_1 + \beta_2 + \beta_3)}{3}$ and $f = \frac{(f_1 + f_2 + f_3)}{3}$ are the average mass fractionation factors from the three sequences.

$\beta_i = \ln\{(0.7219) / (^{146}\text{Nd}/^{144}\text{Nd})_i\} / \ln(145.913126/143.910096)$.

$f_i = \{(0.7219) / (^{146}\text{Nd}/^{144}\text{Nd})_i\}^{1/(145.913126-143.910096)} - 1$.

$i = 1, 2, 3$ which refers to the sequence number.

Table 3
Cup configuration and run conditions used in this study for Nd isotopic ratios measurements on a Triton.

a) Three-sequence method												
Cup	L4	L3	L2	L1	C	H1	H2	H3	H4	Zoom optics		
										Integration time [sec]	Focus [V]	Dispersion [V]
Sequence 1	¹⁴⁰ Ce	¹⁴² Nd	¹⁴³ Nd ¹⁴² Nd	¹⁴⁴ Nd ¹⁴³ Nd ¹⁴² Nd	¹⁴⁵ Nd ¹⁴⁴ Nd ¹⁴³ Nd	¹⁴⁶ Nd ¹⁴⁵ Nd ¹⁴⁴ Nd	¹⁴⁷ Sm ¹⁴⁶ Nd ¹⁴⁵ Nd	¹⁴⁸ Nd ¹⁴⁷ Sm ¹⁴⁶ Nd	¹⁵⁰ Nd ¹⁴⁹ Sm ¹⁴⁸ Nd	8.389 8.389 8.389	0.0 0.0 0.0	0.0 6.0 8.0
Sequence 2												
Sequence 3												
b) Two-sequence method												
Cup	L4	L3	L2	L1	C	H1	H2	H3	H4	Zoom optics		
										Integration time [sec]	Focus [V]	Dispersion [V]
Sequence 1	¹⁴⁰ Ce	¹⁴² Nd	¹⁴³ Nd	¹⁴⁴ Nd ¹⁴² Nd	¹⁴⁵ Nd ¹⁴³ Nd	¹⁴⁶ Nd ¹⁴⁴ Nd	¹⁴⁷ Sm ¹⁴⁵ Nd	¹⁴⁸ Nd ¹⁴⁶ Nd	¹⁵⁰ Nd ¹⁴⁸ Nd	8.389 8.389	0.0 0.0	0.0 8.0
Sequence 2												

Note: Number of blocks = 54, No. of cycles per block = 10, Amplifier rotation to left, Baseline after every 2 blocks, Peak centring after every 8 blocks, Lens focusing after every 4 blocks, No. of integrations = 1, Idle time (sec) = 3, Cycles filtered at 2σ.

law of fractionation correction (e.g., exponential vs. power law). The protocol followed by Roth et al. (2014b) was grossly different from that of Upadhyay et al. (2009). The details are given in Tables 1 and 2.

It is therefore, important that we understand the role of the fractionation correction in the accuracy of ¹⁴²Nd/¹⁴⁴Nd isotopic data and its contribution (if any) to the generation of the analytical artefacts. To study these aspects and to further investigate the accuracy of the negative μ¹⁴²Nd anomalies reported in the alkaline silicate rocks of the Khariar complex, India (Upadhyay et al., 2009), we analysed samples re-collected from the same geological outcrops for their Nd isotopic compositions applying different fractionation correction procedures. We followed identical experimental procedure as in the original study of Upadhyay et al. (2009) and that proposed later by Roth et al. (2014b). Experimental details are provided in Table 3. Both the techniques were evaluated in light of over correction of ¹⁴²Nd/¹⁴⁴Nd resulting from excessive fractionation correction.

2. Samples and methods

The GPS locations of the four samples collected by us are given in Table S-1 of the Supplementary Information. The samples collected by us are geochemically similar to that presented in the original study, the details of which are provided in the Supplementary Information (Fig. S-1(a), (b) and S-2; Table S-2). The samples were powdered using a tungsten carbide mill and processed for chemical separation of Nd followed by isotopic ratio measurements using TIMS. Four samples with four replicates each were processed. Each replicate is a separate dissolution, passed through column and loaded on filament as an independent sample. Out of four replicates, two replicates were analysed for ¹⁴²Nd/¹⁴⁴Nd using 3-sequence multi-dynamic data acquisition scheme of Upadhyay et al. (2009) and the other two replicates using 2-sequence multi-dynamic scheme of Roth et al. (2014b); (Table 3). About ~100 mg of sample powder was dissolved in a concentrated mixture of HF and HNO₃ (2:1). Complete dissolution was achieved through ~1 h of ultra-sonication and heating at 60 °C with closed cap for ~12 h. After two rounds of 8 N HNO₃ treatment and drying, the sample was converted to chloride form using 6 N HCl and the final solution was prepared in 1 ml of 1 N HCl for column chemistry. Rare Earth Elements (REEs) were separated from the rock matrix using A-G*50W-X8 cation exchange resin (200–400 mesh) with 6 N HCl as an elutant. Nd was separated from Sm using Ln-spec resin (50–100 μm) from Eichrom® with 0.3N HCl as elutant. This step was repeated twice to effectively remove all Sm from Nd cut. Effective removal of Ce from Nd was achieved by using AG*50W-X4 resin (200–400 mesh) with 0.15 M alpha-Hydroxyisobutyric Acid (α-HIBA) at a pH of 4.8 as elutant. To remove α-HIBA from the collected Nd, the eluate was heated with concentrated HNO₃ followed by aqua-regia treatment at 150 °C. Total procedural Nd blank was < 120 pg.

Neodymium was measured as Nd⁺ ions on a Triton TIMS at the Department of Earth Sciences, Pondicherry University, India. Nearly 400 ng of Nd was loaded on to the degassed zone refined Re double filament assembly. The evaporation filament was heated to 1000–1500 mA, at a rate of 20 mA/min and the ionization filament to 4000–4300 mA, at a rate of 150 mA/min. This heating of the filaments was carried out in two steps. The first step involved heating of ionization filament to 3500 mA while evaporation filament was heated to 800 mA. Once the ionization filament reaches 3500 mA, in the second step heating of the evaporation filament was resumed. The Nd⁺ signal for 142 mass appeared only after the evaporation filament reached 1000 mA and the corresponding ionization filament current was 4000 mA. The data acquisition was started when Nd⁺ (for 142 mass) reached about 2.5–4.0 V ($R = 10^{11} \Omega$). The Nd was maintained in a window of 80% to 200% of the original signal using Triton software. Details of the run conditions and the fractionation laws used are given in Tables 3 and 2, respectively. Ames Nd standard was analysed (using both 3- and 2- sequence modes; Table 4) as the terrestrial reference for

Table 4
Nd isotopic ratios of AMES standard analysed during the course of our experiment.

Data for three sequence method – corrected for fractionation using power law normalised exponential law										
Sr. No.	$^{142}\text{Nd}/^{144}\text{Nd}$	$\mu^{142}\text{Nd}$	$^{143}\text{Nd}/^{144}\text{Nd}$	$^{145}\text{Nd}/^{144}\text{Nd}$	$\mu^{145}\text{Nd}$	$^{146}\text{Nd}/^{144}\text{Nd}$	$^{148}\text{Nd}/^{144}\text{Nd}$	$\mu^{148}\text{Nd}$	$^{150}\text{Nd}/^{144}\text{Nd}$	Average
1	1.1418373 (56)	-0.2	0.5119596 (18)	0.3484052 (12)	4.3	0.2415821 (16)	9.9	0.2364556 (18)	12.7	0.05
2	1.1418373 (90)	-0.1	0.5119586 (30)	0.3484037 (20)	0.0	0.2415791 (26)	-2.5	0.2364587 (30)	25.8	0.10
3	1.1418332 (56)	-3.8	0.5119581 (18)	0.3484045 (12)	2.3	0.2415805 (16)	3.3	0.2364532 (18)	2.5	0.06
4	1.1418288 (58)	-7.6	0.5119594 (20)	0.3484034 (12)	-0.9	0.2415802 (16)	2.1	0.2364631 (18)	44.4	0.10
5	1.1418426 (48)	4.5	0.5119590 (16)	0.3484032 (10)	-1.4	0.2415765 (14)	-13.2	0.2364502 (16)	-10.2	0.08
6	1.1418393 (64)	1.6	0.5119611 (20)	0.3484046 (14)	2.6	0.2415794 (18)	-1.2	0.2364504 (20)	-9.3	0.04
7	1.1418417 (56)	3.7	0.5119596 (16)	0.3484035 (12)	-0.6	0.2415795 (16)	-0.8	0.2364488 (18)	-16.1	0.04
8	1.1418311 (48)	-5.6	0.5119591 (16)	0.3484044 (10)	2.0	0.2415799 (14)	0.8	0.2364493 (16)	-14.0	0.03
9	1.1418370 (64)	-0.4	0.5119588 (22)	0.3484020 (14)	-4.9	0.2415808 (20)	4.6	0.2364560 (20)	14.4	0.09
10	1.1418376 (44)	0.1	0.5119582 (14)	0.3484044 (10)	2.0	0.2415801 (14)	1.7	0.2364518 (14)	-3.4	0.06
11	1.1418405 (46)	2.6	0.5119574 (16)	0.3484033 (10)	-1.1	0.2415788 (10)	-3.7	0.2364509 (16)	-7.2	0.05
12	1.1418363 (44)	-1.1	0.5119587 (14)	0.3484044 (10)	2.0	0.2415796 (14)	-0.4	0.2364525 (14)	-0.4	0.05
13	1.1418365 (48)	-0.9	0.5119588 (16)	0.3484034 (10)	-0.9	0.2415800 (12)	1.2	0.2364479 (16)	-19.9	0.10
14	1.1418413 (62)	3.3	0.5119572 (18)	0.3484025 (14)	-3.4	0.2415799 (18)	0.8	0.2364491 (20)	-14.8	0.05
15	1.1418421 (58)	4.0	0.5119568 (18)	0.3484023 (12)	-4.0	0.2415793 (16)	-1.7	0.2364517 (18)	-3.8	0.04
Average	1.1418375		0.5119587	0.3484037		0.2415797		0.2364526		
2RSD (ppm)	0.0000071		0.0000042	0.0000053		0.0000099		0.0000352		

(b) Data for two sequence method – corrected for fractionation using simple exponential law

Data for two sequence method – corrected for fractionation using simple exponential law										
Sr. No.	$^{142}\text{Nd}/^{144}\text{Nd}$	$\mu^{142}\text{Nd}$	$^{143}\text{Nd}/^{144}\text{Nd}$	$^{145}\text{Nd}/^{144}\text{Nd}$	$\mu^{145}\text{Nd}$	$^{146}\text{Nd}/^{144}\text{Nd}$	$^{148}\text{Nd}/^{144}\text{Nd}$	$\mu^{148}\text{Nd}$	$^{150}\text{Nd}/^{144}\text{Nd}$	Average
1	1.1418353 (60)	-3.2	0.5119636 (28)	0.3484037 (16)	0.9	0.2415894 (20)	20.3	0.2364629 (27)	44.0	0.01
2	1.1418414 (76)	2.1	0.5119614 (36)	0.3484022 (22)	-3.4	0.2415820 (26)	-10.3	0.2364479 (34)	-19.5	0.02
3	1.1418355 (61)	-3.1	0.5119622 (28)	0.3484031 (19)	-0.9	0.2415821 (21)	-9.9	0.2364494 (27)	-13.1	0.04
4	1.1418374 (54)	-1.4	0.5119639 (26)	0.3484017 (16)	-4.9	0.2415905 (19)	24.8	0.2364600 (25)	31.7	0.004
5	1.1418371 (54)	-1.7	0.5119645 (25)	0.3484051 (16)	4.9	0.2415840 (19)	-2.1	0.2364506 (26)	-8.0	0.03
6	1.1418355 (57)	-3.1	0.5119636 (27)	0.3484038 (17)	1.1	0.2415841 (20)	-1.7	0.2364507 (26)	-7.6	0.02
7	1.1418330 (69)	-5.3	0.5119669 (32)	0.3484023 (20)	-3.2	0.2415852 (23)	2.9	0.2364515 (32)	-4.2	0.05
8	1.1418388 (57)	-0.2	0.5119662 (28)	0.3484060 (17)	7.5	0.2415833 (19)	-5.0	0.2364489 (28)	-15.2	0.06
9	1.1418436 (136)	4.0	0.5119671 (64)	0.3484030 (41)	-1.1	0.2415812 (48)	-13.7	0.2364492 (66)	-14.0	0.10
10	1.1418393 (50)	0.3	0.5119649 (24)	0.3484023 (15)	-3.2	0.2415840 (18)	-2.1	0.2364531 (23)	2.5	0.03
11	1.1418376 (53)	-1.2	0.5119647 (27)	0.3484024 (16)	-2.9	0.2415819 (18)	-10.8	0.2364493 (24)	-13.5	0.06
12	1.1418426 (56)	3.2	0.5119643 (26)	0.3484042 (16)	2.3	0.2415815 (19)	-12.4	0.2364494 (24)	-13.1	0.09
13	1.1418364 (50)	-2.3	0.5119634 (26)	0.3484050 (14)	4.6	0.2415889 (18)	18.2	0.2364620 (23)	40.2	0.05
14	1.1418334 (52)	-4.9	0.5119649 (23)	0.3484025 (15)	-2.6	0.2415882 (17)	15.3	0.2364598 (24)	30.9	0.06
15	1.1418460 (54)	6.1	0.5119666 (26)	0.3484036 (16)	0.6	0.2415842 (19)	-1.2	0.2364492 (25)	-14.0	0.10
16	1.1418486 (58)	8.4	0.5119664 (27)	0.3484064 (17)	8.6	0.2415833 (20)	-5.0	0.2364496 (27)	-12.3	0.03
17	1.1418320 (46)	-6.1	0.5119624 (20)	0.3484011 (13)	-6.6	0.2415842 (15)	-1.2	0.2364496 (20)	-12.3	0.10
18	1.1418482 (52)	8.1	0.5119675 (25)	0.3484026 (16)	-2.3	0.2415833 (18)	-5.0	0.2364520 (23)	-2.1	0.10
Average	1.1418390		0.5119647	0.3484034		0.2415845		0.2364525		
2RSD (ppm)	0.0000089		0.0000070	0.0000085		0.0000235		0.0000420		

Table 5
Nd isotopic ratio data for Khariar samples analysed in this work.

Sample ID	Method	$^{142}\text{Nd}/^{144}\text{Nd}$	$\mu^{142}\text{Nd}$	$^{143}\text{Nd}/^{144}\text{Nd}$	$^{145}\text{Nd}/^{144}\text{Nd}$	$^{148}\text{Nd}/^{144}\text{Nd}$	$^{150}\text{Nd}/^{144}\text{Nd}$	$^{140}\text{Ce}/^{142}\text{Nd}$	Av. Fr. Rate (ppm/s)
OD-8/1									
(1)	3- sequence	1.1418219 (38)	− 13.7	0.5116305 (12)	0.3484050 (9)	0.2415817 (11)	0.2364475 (13)	1.08E-04	0.02
(2)	3- sequence	1.1418311 (41)	− 5.6	0.5116324 (146)	0.3484047 (8)	0.2415802 (11)	0.2364510 (13)	8.31E-05	0.08
Average		1.1418265 (130)	− 9.6	0.5116315 (27)	0.3484049 (4)	0.2415810 (21)	0.2364493 (49)		
(3)	2- sequence	1.1418298 (42)	− 8.1	0.5116386 (19)	0.3484049 (12)	0.2415835 (14)	0.2364485 (19)	9.25E-05	0.05
(4)	2- sequence	1.1418312 (45)	− 6.8	0.5116380 (21)	0.3484037 (13)	0.2415847 (15)	0.2364516 (20)	2.07E-05	0.06
Average		1.1418305 (20)	− 7.4	0.5116383 (8)	0.3484043 (17)	0.2415841 (17)	0.2364501 (44)		
OD-7/1									
(1)	3- sequence	1.1418272 (41)	− 9.0	0.5116740 (12)	0.3484036 (9)	0.2415803 (12)	0.2364503 (13)	5.47E-05	0.08
(2)	3- sequence	1.1418389 (49)	1.2	0.5116776 (15)	0.3484044 (10)	0.2415799 (15)	0.2364546 (17)	1.25E-05	0.06
Average		1.1418331 (165)	− 3.9	0.5116758 (51)	0.3484040 (11)	0.2415801 (6)	0.2364525 (61)		
(3)	2- sequence	1.1418304 (41)	− 7.5	0.5116803 (19)	0.3484049 (11)	0.2415828 (14)	0.2364504 (19)	3.56E-05	0.10
(4)	2- sequence	1.1418322 (47)	− 6.0	0.5116812 (21)	0.3484066 (14)	0.2415869 (16)	0.2364559 (23)	3.29E-05	0.07
Average		1.1418313 (25)	− 6.7	0.5116808 (13)	0.3484058 (24)	0.2415849 (58)	0.2364532 (78)		
OD-6/1									
(1)	3- sequence	1.1418226 (57)	− 13.0	0.5116595 (18)	0.3484044 (12)	0.2415815 (16)	0.2364463 (19)	8.28E-05	0.01
(2)	3- sequence	1.1418309 (45)	− 5.8	0.5116573 (14)	0.3484044 (10)	0.2415809 (12)	0.2364554 (14)	6.76E-05	0.02
Average		1.1418268 (117)	− 9.4	0.5116584 (31)	0.3484044 (0)	0.2415812 (8)	0.2364509 (129)		
(3)	2- sequence	1.1418290 (40)	− 8.8	0.5116601 (20)	0.3484056 (11)	0.2415811 (13)	0.2364488 (18)	5.98E-05	0.10
(4)	2- sequence	1.1418382 (41)	− 0.7	0.5116611 (17)	0.3484064 (11)	0.2415876 (14)	0.2364583 (18)	7.68E-05	0.02
Average		1.1418336 (130)	− 4.7	0.5116606 (14)	0.3484060 (11)	0.2415844 (92)	0.2364536 (134)		
OD-3/3									
(1)	3- sequence	1.1418269 (40)	− 9.3	0.5115282 (11)	0.3484051 (8)	0.2415813 (11)	0.2364546 (13)	6.48E-05	0.02
(4)	3- sequence	1.1418239 (37)	− 11.9	0.5115335 (11)	0.3484048 (7)	0.2415809 (11)	0.2364506 (12)	1.20E-05	0.02
Average		1.1418254 (42)	− 10.6	0.5115309 (75)	0.3484050 (4)	0.2415811 (6)	0.2364526 (57)		
(2)	2- sequence	1.1418311 (43)	− 6.9	0.5115413 (19)	0.3484050 (12)	0.2415877 (15)	0.2364580 (20)	8.09E-05	0.01
(3)	2- sequence	1.1418332 (39)	− 5.1	0.5115408 (19)	0.3484023 (12)	0.2415853 (15)	0.2364546 (18)	2.13E-05	0.08
Average		1.1418322 (30)	− 6.0	0.5115411 (7)	0.3484037 (38)	0.2415865 (34)	0.2364563 (48)		
BHVO-2									
(A)	3- sequence	1.1418246 (52)	− 11.3	0.5129695 (16)	0.3484046 (12)	0.2415814 (15)	0.2364523 (17)	7.60E-05	0.08
(C)	3- sequence	1.1418444 (57)	6.04	0.5129723 (19)	0.3484034 (13)	0.2415797 (17)	0.2364513 (18)	1.79E-05	0.04
Average		1.1418345 (279)	− 2.63	0.5129709 (39)	0.3484040 (18)	0.2415805 (24)	0.2364518 (14)		
(B)	2- sequence	1.1418365 (49)	− 2.19	0.5129762 (21)	0.3484053 (13)	0.2415834 (16)	0.2364470 (22)	1.49E-04	0.07
(B)-2	2- sequence	1.1418339 (42)	− 4.47	0.5129732 (19)	0.3484057 (13)	0.2415858 (14)	0.2364533 (19)	2.70E-05	0.08
(C)-2	2- sequence	1.1418403 (45)	1.14	0.5129763 (20)	0.3484036 (12)	0.2415841 (15)	0.2364526 (20)	6.80E-05	0.20
Average		1.1418369 (64)	− 1.84	0.5129753 (35)	0.3484049 (22)	0.2415844 (24)	0.2364510 (69)		

Note: 3-sequence and 2-sequence $\mu^{142}\text{Nd}$ values were determined using AMES Nd standard $^{142}\text{Nd}/^{144}\text{Nd}$ of 1.1418375 and 1.4148390, respectively. It should be noted that the 3-sequence data have been corrected for mass fractionation using a power-normalized exponential law, whereas that of 2-sequence using exponential law. The internal precision (2SE) is given in parentheses. For average values, 2 standard-deviations (2SD) are given in the parentheses. Av. Fr. Rate = Average Fractionate Rate = slope of the linear regression in a plot of $^{146}\text{Nd}/^{144}\text{Nd}$ from the first sequence versus time.

calculation of $\mu^{142}\text{Nd}$ of samples. For the 3-sequence data acquisition scheme, each run lasted for about 6–7 h and that for the 2-sequence data acquisition scheme, around 5 h. Isobaric interferences on Nd isotopes from Sm and Ce were monitored by measuring ^{147}Sm and ^{140}Ce , respectively. The $^{140}\text{Ce}/^{142}\text{Nd}$ for the analysed samples is given in Table 5. The maximum and minimum values of $^{140}\text{Ce}/^{142}\text{Nd}$ were 1.49×10^{-4} and 1.20×10^{-5} , respectively. $^{147}\text{Sm}/^{144}\text{Nd}$ values never exceeded 7.65×10^{-7} and hence deemed insignificant for any correction. Nonetheless, interference corrections for Ce and Sm were applied for the standard and samples. We did not see any significant correlation between the $^{140}\text{Ce}/^{142}\text{Nd}$ and the corresponding fractionation corrected $^{142}\text{Nd}/^{144}\text{Nd}$ (Fig. S-3; Supplementary Information). This lack of correlation suggests that the interference corrections applied for Ce and Sm did not bias the final ^{142}Nd data, therefore were robust.

3. Results

In this study we have used Ames Nd standard for normalization of $^{142}\text{Nd}/^{144}\text{Nd}$ of samples, because it was routinely analysed along with the samples. We have also analysed JNdi-1 standard and Nd from rock standard BHVO-2 for accuracy check. All standards and samples of alkaline silicate rocks from Khariar were analysed using multi-dynamic scheme of data acquisition employing both 3- and 2-sequence modes. Fifteen and eighteen loads of Ames Nd were analysed for the 3-

sequence and 2- sequence modes, respectively. In the 3-sequence mode, isotopic ratios were corrected for mass fractionation using the *power (law)-normalised exponential law* as in Upadhyay et al. (2009) and our experiment yielded an average value of 1.1418375 for $^{142}\text{Nd}/^{144}\text{Nd}$ of Ames Nd with an external reproducibility of 7.1 ppm (Table 4-a). In the 2-sequence mode, the simple *exponential fractionation law* (as in Roth et al., 2014b) was used and an average value of 1.1418390 for $^{142}\text{Nd}/^{144}\text{Nd}$ was obtained with an external reproducibility of 8.9 ppm (Table 4-b). Our external precision (2 SD) is lower than that reported by most studies on such experiments (i.e., ~5 ppm), in spite of the fact that the within-run precisions are < 5 ppm (2 SE). The reason for the lower external precision could be because of the aging (> 12 years old) of the Faraday Cups.

Because we have used two different schemes of data acquisition for the samples and BHVO-2, the above two values of $^{142}\text{Nd}/^{144}\text{Nd}$ for Ames Nd have been used for determination of $\mu^{142}\text{Nd}$ (Figs. 1 and 2). $\mu^{142}\text{Nd}$ values of Khariar samples obtained through a 3-sequence method appear to be slightly negative, albeit unresolvable within 2SD, compared to those obtained through a 2-sequence method (Figs. 1 and 2). It should be noted that the average fractionation rates (r_a), irrespective of the number of sequences, are less than the threshold fractionation rates (r_f) (Table 5).

To understand the role of fractionation correction in the generation of analytical artefacts, the raw/uncorrected data for 67 Ames Nd

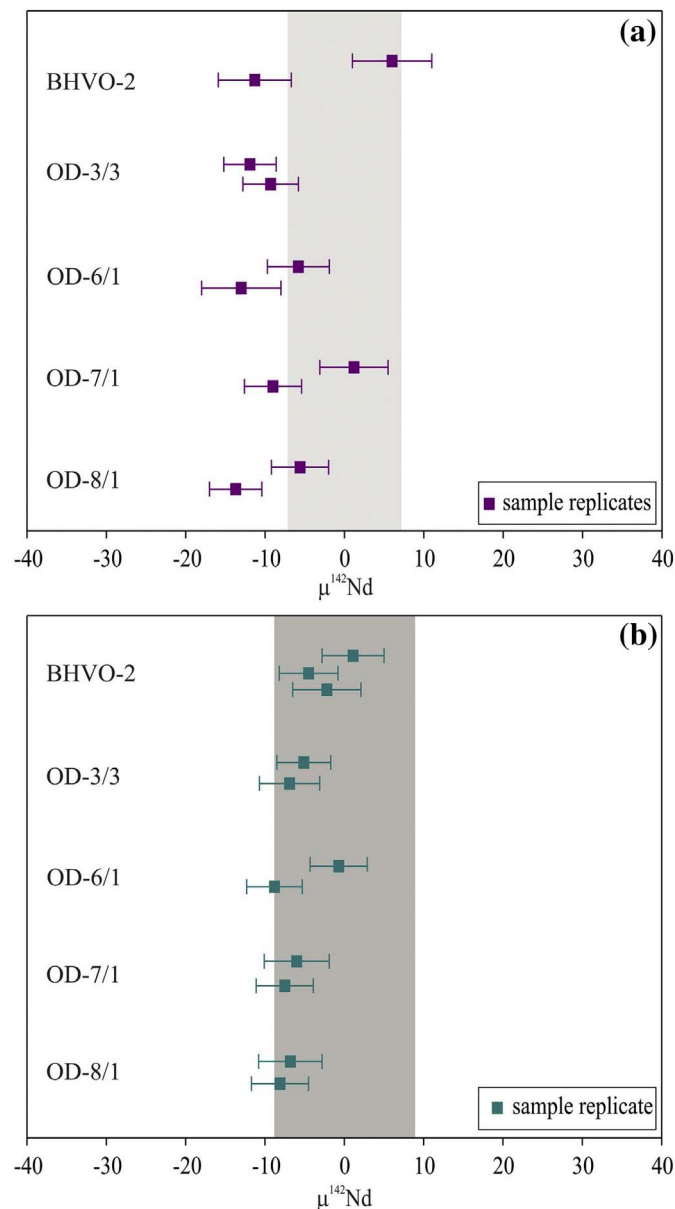


Fig. 1. $\mu^{142}\text{Nd}$ values of 1.48 Ga alkaline rocks from Khariar analysed in this study: (a) data acquired using a 3-sequence multi dynamic mode and corrected for mass fractionation using the *power-normalised exponential law*; (b) data acquired using a 2-sequence multi dynamic mode and corrected for mass fractionation using the *exponential law*. The average values of Ames Nd used for calculating $\mu^{142}\text{Nd}$ in (a) and (b) are 1.1418375 ± 7.1 ppm (2RSD, $n = 15$) and 1.1418390 ± 8.9 ppm (2RSD, $n = 18$), respectively. The grey bands encompass $\pm 2\text{RSD}$, external reproducibility, for Ames Nd standard.

aliquots (Table S-3), analysed during and prior to this experiment over a period of 3 years, were corrected for mass fractionation using the (1) *power-normalised exponential law*, and (2) *exponential law*. Data acquired using 2-sequence mode were not included in this exercise, because barring $^{142}\text{Nd}/^{144}\text{Nd}$ all other Nd isotopic ratios cannot be corrected for fractionation using the first law (i.e. 1; Tables 1 and 2). Figs. 3 and 4 show results of this exercise. The average values for $^{142}\text{Nd}/^{144}\text{Nd}$, $^{143}\text{Nd}/^{144}\text{Nd}$, $^{145}\text{Nd}/^{144}\text{Nd}$, $^{148}\text{Nd}/^{144}\text{Nd}$ and $^{150}\text{Nd}/^{144}\text{Nd}$ are given in Table S-3 along with their respective 2SD values. Eleven aliquots of JNdi-1 were analysed along with six loads of Ames Nd (Table 6; Fig. 5). As can be seen in Fig. 5 all Nd isotopic ratios of JNdi-1, although overlap at 2SD with those of the Ames standard, show minor differences in the mean values. The average value of $^{142}\text{Nd}/^{144}\text{Nd}$ for JNdi-1 is

lower by 6 ppm compared to that of the long term average of Ames Nd (Fig. S-4). Consequently, $\mu^{142}\text{Nd}$ values of Khariar samples calculated using $^{142}\text{Nd}/^{144}\text{Nd}$ of JNdi-1 lost their apparent deficit from normal (Fig. 6). It should be noted that for comparison we have used isotopic ratios of $^{142}\text{Nd}/^{144}\text{Nd}$ instead of $\mu^{142}\text{Nd}$ in Fig. 6.

4. Discussion

High precision isotopic ratio measurements by TIMS often requires data acquisition through a multi-dynamic mode, wherein differences in collector efficiencies/factors can be nullified by measuring individual ion beams in multiple Faraday Cups through peak jumping. In such a data acquisition method, the *power-normalised exponential law* is

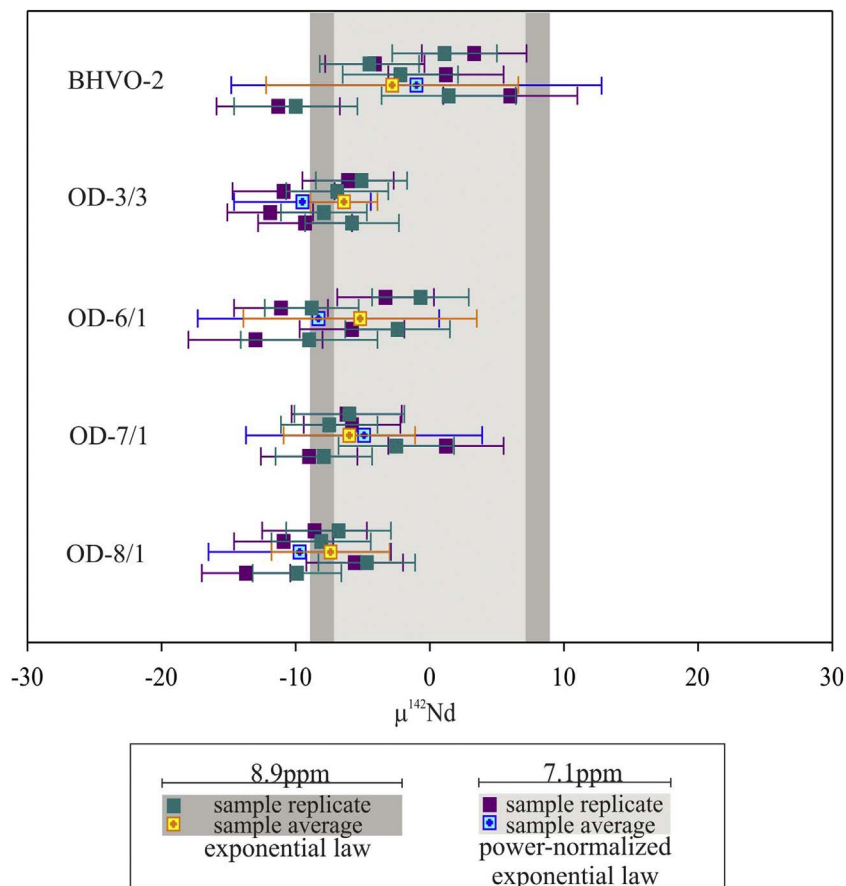


Fig. 2. $\mu^{142}\text{Nd}$ of Khariar rocks and BHVO-2, analysed in this study, with respect to the Ames Nd. The data acquired in both 3- and 2-sequences are corrected offline for mass fractionation using both the *power-normalised exponential law* and the *exponential law*. The average values of four replicates for each sample are also plotted with errors; 2SE for individual analyses and 2SD for the average values (Table 5). The external reproducibility (2RSD) for the Ames Nd standard is 7.1 ppm for *power-normalised exponential law* (inner light grey band) and 8.9 ppm for *exponential law* (outer dark grey band).

deemed as the most appropriate method for correction of machine induced mass fractionation (Thirlwall, 1991; Supplementary Information). Whereas Upadhyay et al. (2009) followed the above fractionation correction method to discover $\mu^{142}\text{Nd}$ anomalies in Khariar alkaline rocks, Roth et al. (2014b) used the simple *exponential law*, generally used in static mode of data acquisition, and rejected the claim of Upadhyay et al. (2009). Our experimentation was aimed at comparing both the methods. Our results, presented above, are discussed below exploring the effects of (1) rate of mass fractionation, (2) choice of law of fractionation correction, and (3) choice of terrestrial standard.

4.1. Rate of mass fractionation

Following Roth et al. (2014b), we have calculated and compared threshold (r_t), average (r_a) and relative (r_f) rates of fractionation for both 3- and 2-sequence multi-dynamic modes. If the external precision for $^{142}\text{Nd}/^{144}\text{Nd}$ measurements were considered to be 5 ppm, then the respective r_t values would have been 0.22 ppm/s and 0.44 ppm/s for corresponding time durations of 22.8 s and 11.4 s, respectively. Our isotopic data from all the analyses of samples and standards, by both modes, show $r_a < 0.22$ ppm/s (Tables 4, 5 and S-3), suggesting $r_f < 1$. This is unlike what Roth et al. (2014b) observed in the 3-sequence data of Upadhyay et al. (2009), i.e., $r_f > 1$. Consequently, there was no need for the time correction in the data acquired in our 3-sequence mode to deal with any excess fractionation. Therefore, we infer that the time-gaps between successive sequences in a multi-dynamic mode do not affect the quality of the data acquired (when $r_a < r_t$).

4.2. Correction for mass fractionation

A comparison of the pattern of mass fractionation observed in our data with the theoretical patterns expected from various empirical fractionation laws (Habfast, 1998), with the help of $^{142}\text{Nd}/^{144}\text{Nd}$ versus $^{150}\text{Nd}/^{144}\text{Nd}$, reveals that the *exponential law* best explains the observed pattern in each individual sequences (Fig. 7), which are equivalent to static mode of data acquisitions. The same method was utilized by Roth et al. (2014b) during the reanalysis of Upadhyay et al. (2009) samples in their 2- sequence mode of data acquisition. As mentioned in Section 3, we have corrected the raw data for Ames Nd, acquired through a 3-sequence mode, using both the *power-normalised exponential law* and the *exponential law* (Table S-3; Figs. 3 and 4). The details of the laws and correction procedure adapted by us are discussed in detail in the Section-S2 in the Supplementary Information and Table 2, respectively. We observe that: (1) isotopic ratios corrected using the *power-normalised exponential law* do not show any significant inter correlation (Figs. 3a–d and 4a–d), whereas the *exponential law* correction method leaves behind substantial residual correlations, especially for $^{150}\text{Nd}/^{144}\text{Nd}$ and $^{148}\text{Nd}/^{144}\text{Nd}$ (Figs. 3e–h and 4e–h); (2) *power-normalised exponential law* noticeably improves precisions (2SD) for $^{143}\text{Nd}/^{144}\text{Nd}$ (5.1 ppm), $^{145}\text{Nd}/^{144}\text{Nd}$ (4.6 ppm) and $^{148}\text{Nd}/^{144}\text{Nd}$ (11.7 ppm) ratios, compared to those obtained through *exponential correction* (Table S-3; Figs. 3 and 4), which are 17.4 ppm, 11.7 ppm and 26.5 ppm, respectively. However, the 2SD values for $^{150}\text{Nd}/^{144}\text{Nd}$ are similar in both the methods because it is obtained from only one sequence (i.e., sequence-1), like that in a static mode but with different β values (Tables 1 and 2). Residual correlations as described above, in (1), are undesirable and

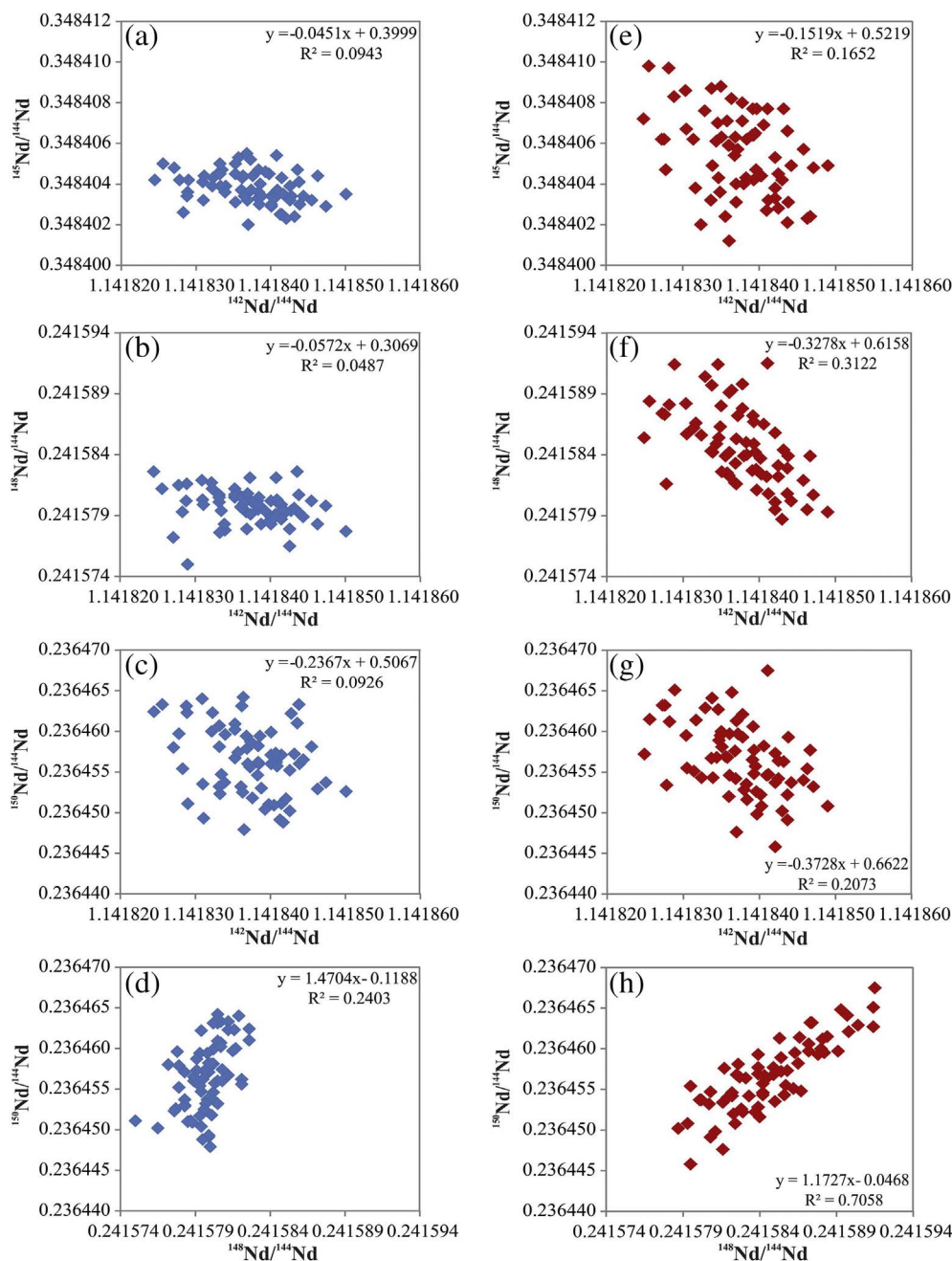


Fig. 3. Plots of Nd isotopic ratios (except for $^{143}\text{Nd}/^{144}\text{Nd}$) for Ames Nd standard ($n = 67$) obtained during 3-sequence data acquisition method (data are in Table S-3 in Supplementary Information). Each datum (raw, corrected only for interference corrections) is corrected offline using the power-normalised exponential law (a–d) as well as the exponential law (e–h).

indicate insufficiency of the method/law used for mass fractionation (Andreasen and Sharma, 2009). We, therefore, infer that application of the power-normalised exponential law for correction of mass dependent fractionation in a multi-dynamic method is the most appropriate data reduction approach.

Using the power-normalised exponential law we corrected data for our samples acquired through both the 3- and 2-sequence modes (Fig. 2), but could not reproduce the anomalies of Upadhyay et al. (2009). We, however, observed that the mean $\mu^{142}\text{Nd}$ values of some of the sample-replicates plotted outside, on the negative side, the 7.1 ppm range defined for the standard (also corrected using the power-normalised

exponential law). In contrast, sample data from both 3- and 2-sequence modes corrected using the exponential law plotted well within the 8.9 ppm range for the standard, corrected using the exponential law (Fig. 2). In addition to $\mu^{142}\text{Nd}$, inter comparison was also done for stable Nd isotopic compositions acquired through 3-sequence mode and corrected using both the laws (Figs. S-5 and S-6). As can be seen data corrected using the exponential law show larger spread compared to those corrected using the power-normalised exponential law (Figs. S-5 and S-6). It is therefore evident that it is the method of fractionation correction and not the mode of data acquisition that controls the quality of data.

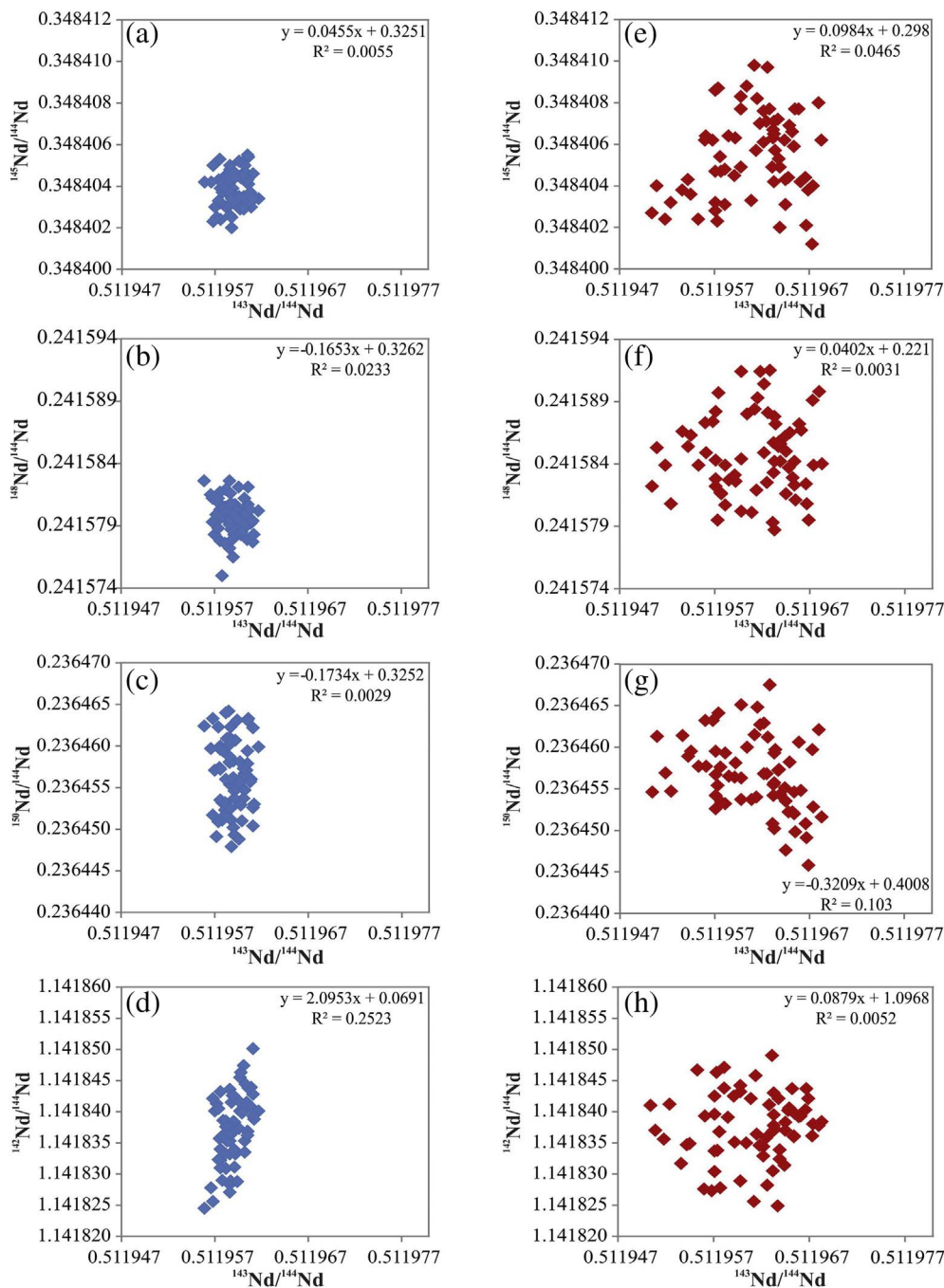


Fig. 4. $^{143}\text{Nd}/^{144}\text{Nd}$ isotopic ratio of Ames Nd is compared with the other Nd isotopic ratios ($n = 67$). The data was acquired during 3-sequence method (Table S-3) and corrected offline for mass fractionation using both the laws, i.e. power-normalised exponential law (a – d) and exponential law (e – h).

4.3. Choice of the terrestrial standard

Because the $^{142}\text{Nd}/^{144}\text{Nd}$ isotopic ratio of the terrestrial standard is key to the definition of $\mu^{142}\text{Nd}$ and therefore, to any discovery of anomalous compositions, it is essential that the standard should possess uniform isotopic ratio and truly represent the modern accessible mantle. Several terrestrial standards have been used over the years in ^{142}Nd studies- such as LaJolla Nd, JNdi-1, Ames Nd and many in-house standards. Although it is expected that all the stable Nd isotopic ratios and $^{142}\text{Nd}/^{144}\text{Nd}$ of these standards are identical, observations suggest otherwise (e.g., Brandon et al., 2009; O'Neil et al., 2008; Saji et al., 2016; Wakaki and Tanaka, 2012). This can lead to appearance or disappearance of anomalies depending on choice of the standard. We observed such a phenomenon in our data too, when $^{142}\text{Nd}/^{144}\text{Nd}$ of Khariar samples were normalised with respect to Ames Nd and JNdi-1. The slight negative $\mu^{142}\text{Nd}$ obtained using Ames Nd became

normal with respect to JNdi-1 (Fig. 6). The mean values of $\mu^{142}\text{Nd}$ of BHVO-2 measured by us are different with respect to each standard; however, they overlap within the external reproducibility of each standard (Fig. 6).

It should be noted that Upadhyay et al. (2009) used La Jolla as reference whereas Roth et al. (2014b) used JNdi-1. La Jolla possesses higher $^{142}\text{Nd}/^{144}\text{Nd}$ with respect to JNdi-1 (Wakaki and Tanaka, 2012), similar to what we observe in the case of Ames Nd (Fig. 6; Table 6). We speculate that the conflicting results obtained from the same aliquots of the Khariar samples by Upadhyay et al. (2009) and Roth et al. (2014b) are a combined effect of the choice of fractionation correction law and terrestrial standard used for calculation of μ .

5. Conclusions

This work evaluates the effects of various analytical methods on the

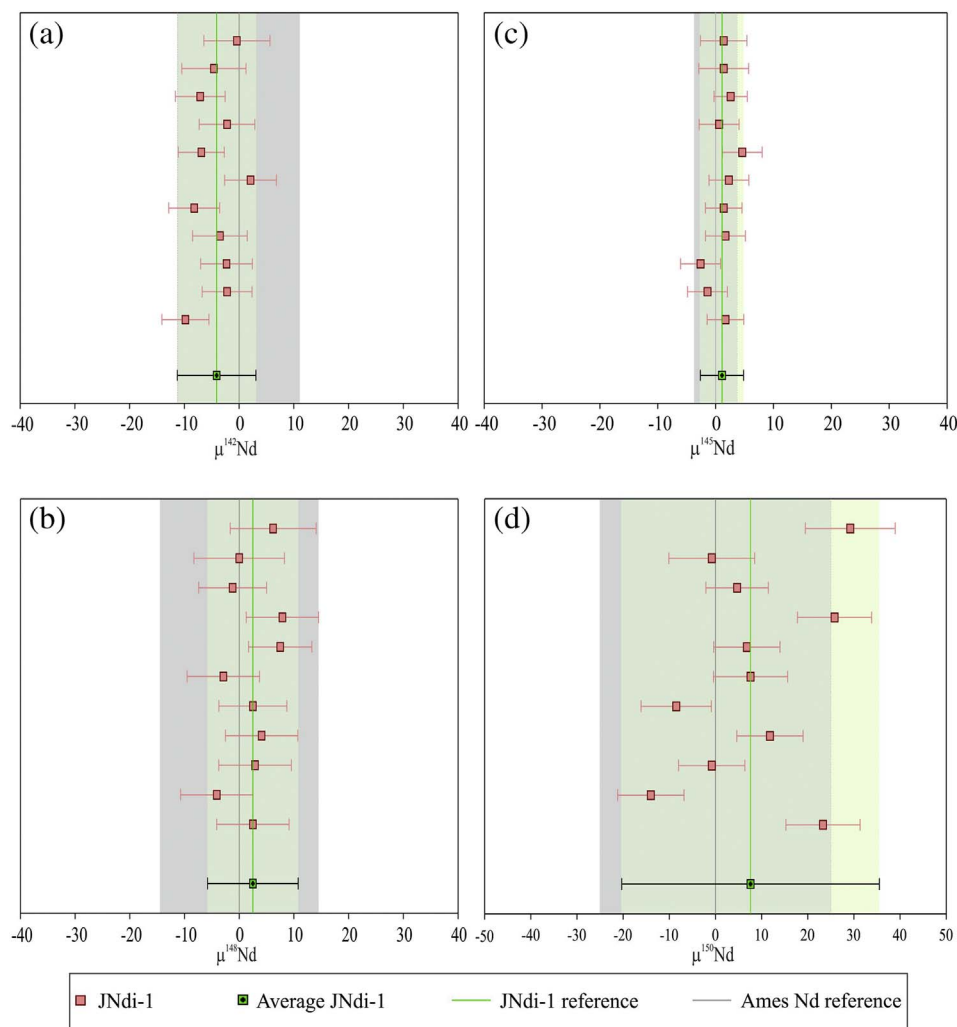


Fig. 5. Comparison of various Nd isotopic compositions of JNdi-1 ($n = 11$) and Ames Nd ($n = 6$) in μ notation. $\mu^i = ((^{145}\text{Nd}/^{144}\text{Nd})_{\text{JNdi-1}} / (^{145}\text{Nd}/^{144}\text{Nd})_{\text{Ames}} - 1) \times 10^6$, where $i = 142, 145, 148$ and 150 . Data are given in Table 6. Pink squares represent individual measurements of the JNdi-1 and green square (cross-haired) represents average value for JNdi-1. The green shaded area shows external reproducibility (2RSD) for JNdi-1 whereas grey shaded area represents the same for Ames Nd. (For interpretation of the references to colour in this figure legend, the reader is referred to the web version of this article.)

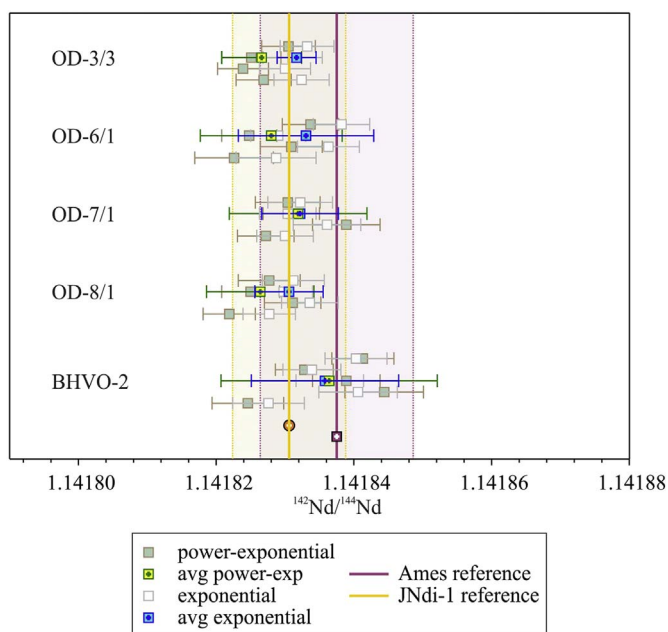


Fig. 6. This plot shows $^{142}\text{Nd}/^{144}\text{Nd}$ of the Khariar alkaline rocks and terrestrial standard BHVO-2 analysed by us, where raw data are corrected for mass fractionation using the *power-normalised exponential law* and the *exponential law*. The reference value for Ames Nd is 1.1418375, whereas for JNdi-1 it is 1.1418306. Pink shaded area shows external reproducibility for Ames Nd (2RSD) and yellow shaded area shows external reproducibility (2RSD) of JNdi-1. (For interpretation of the references to colour in this figure legend, the reader is referred to the web version of this article.)

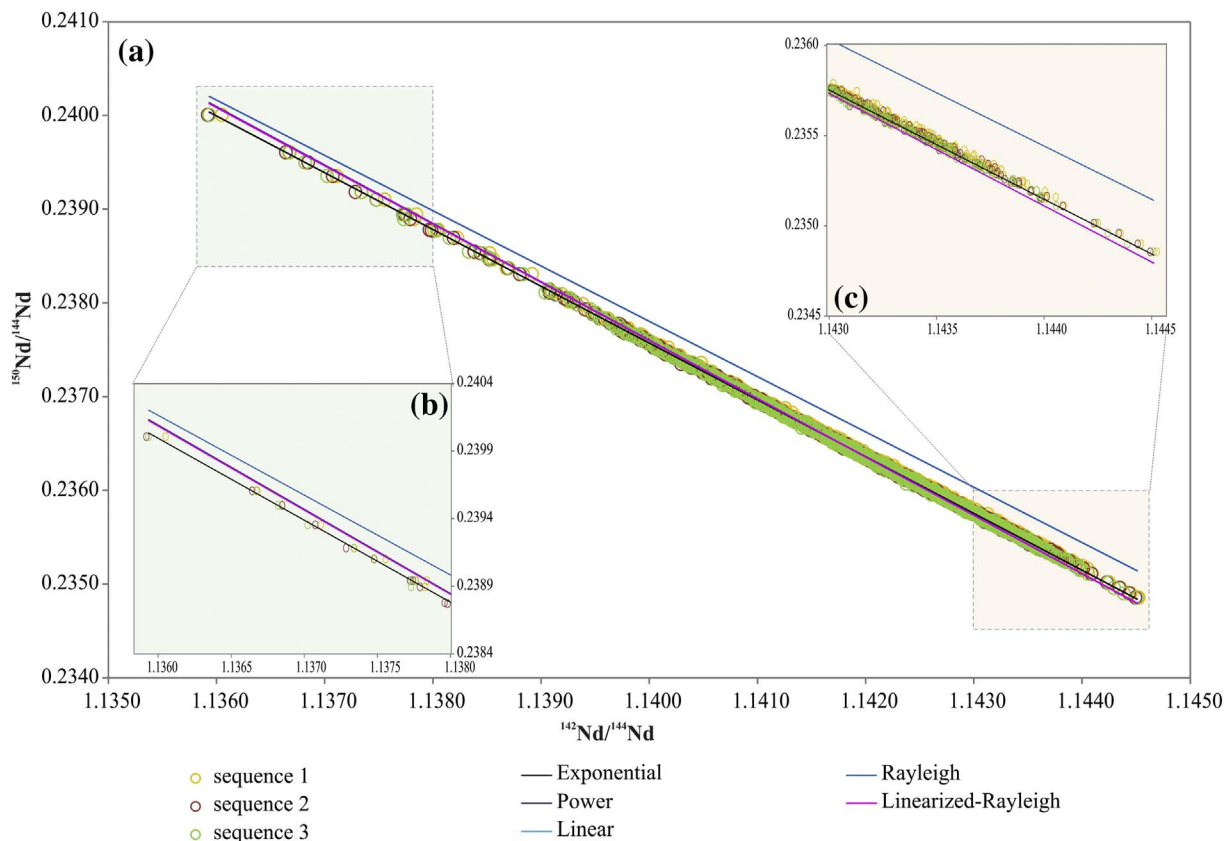


Fig. 7. (a) Plot of uncorrected $^{150}\text{Nd}/^{144}\text{Nd}$ versus $^{142}\text{Nd}/^{144}\text{Nd}$ isotopic ratios for Ames Nd standard acquired using a 3-sequence multi-dynamic mode. $^{142}\text{Nd}/^{144}\text{Nd}$ values are from all the three sequences and $^{150}\text{Nd}/^{144}\text{Nd}$ from the first sequence only. Each point is an average of 10 cycles (one block) and the plot contains data from 752 blocks for 14 analyses. Lines corresponding to different fractionation laws are also shown. (b) and (c) represent enlarged versions of the marked segments of the plot. (For interpretation of the references to colour in this figure legend, the reader is referred to the web version of this article.)

Table 6
Neodymium isotopic ratios of JNdi-1 and Ames analysed with JNdi-1.

Sample ID	$^{142}\text{Nd}/^{144}\text{Nd}$	$^{143}\text{Nd}/^{144}\text{Nd}$	$^{145}\text{Nd}/^{144}\text{Nd}$	$^{148}\text{Nd}/^{144}\text{Nd}$	$^{150}\text{Nd}/^{144}\text{Nd}$
JNdi-1					
091116	1.1418241 (49)	0.5120979 (17)	0.3484048 (11)	0.2415805 (16)	0.2364540 (19)
111116	1.1418328 (52)	0.5120989 (15)	0.3484037 (12)	0.2415789 (16)	0.2364452 (17)
131116	1.1418327 (54)	0.5121015 (16)	0.3484033 (12)	0.2415806 (16)	0.2364483 (17)
181116	1.1418313 (57)	0.5120997 (18)	0.3484048 (12)	0.2415809 (16)	0.2364513 (17)
191116	1.1418259 (53)	0.5120983 (17)	0.3484047 (11)	0.2415805 (15)	0.2364465 (18)
211116	1.1418377 (54)	0.5121003 (17)	0.3484050 (12)	0.2415792 (16)	0.2364503 (19)
181116	1.1418274 (48)	0.5120976 (15)	0.3484058 (12)	0.2415817 (14)	0.2364501 (17)
211116	1.1418328 (58)	0.5121000 (19)	0.3484044 (12)	0.2415818 (16)	0.2364546 (19)
101116	1.1418272 (52)	0.5120997 (17)	0.3484051 (10)	0.2415796 (15)	0.2364496 (16)
091116	1.1418300 (67)	0.5121006 (23)	0.3484047 (15)	0.2415799 (20)	0.2364483 (22)
221116	1.1418349 (69)	0.5121019 (21)	0.3484047 (14)	0.2415814 (19)	0.2364554 (23)
Average	1.1418306	0.5120997	0.3484046	0.2415805	0.2364503
2SD	0.0000082	0.0000028	0.0000013	0.0000020	0.0000066
Ames Nd					
081116	1.1418269 (54)	0.5119586 (17)	0.3484044 (14)	0.2415819 (17)	0.2364496 (17)
081116	1.1418324 (58)	0.5119571 (18)	0.3484036 (12)	0.2415801 (16)	0.2364490 (18)
101116	1.1418378 (45)	0.5119625 (14)	0.3484052 (11)	0.2415800 (14)	0.2364475 (16)
111116	1.1418339 (51)	0.5119573 (15)	0.3484045 (10)	0.2415816 (14)	0.2364491 (16)
141116	1.1418348 (51)	0.5119585 (17)	0.3484034 (11)	0.2415775 (16)	0.2364435 (17)
141116	1.1418460 (51)	0.5119606 (17)	0.3484039 (11)	0.2415784 (17)	0.2364524 (18)
average	1.1418353	0.5119591	0.3484042	0.2415799	0.2364485
2SD	0.0000127	0.0000042	0.0000013	0.0000035	0.0000059

The data is acquired using three sequence multi dynamic mode and corrected for the fractionation using power-normalised exponential law (normalised to $^{146}\text{Nd}/^{144}\text{Nd} = 0.7219$). Internal precision is given in brackets (2SE). For average values, 2standard deviation (2SD) is given.

accuracy of $^{142}\text{Nd}/^{144}\text{Nd}$ measurements by TIMS and extends this information for the determination of $\mu^{142}\text{Nd}$ of alkaline rocks from Khariar complex, India. The important report of the negative $\mu^{142}\text{Nd}$ anomalies in the 1.48 billion year old alkaline silicate rocks from Khariar complex by Upadhyay et al. (2009) needed independent verifications. Following identical analytical procedures on freshly collected samples from the same outcrops we were unsuccessful in reproducing these anomalies. However, we did observe slightly negative $\mu^{142}\text{Nd}$, although unresolvable, when Ames Nd was the standard for normalization. These negative values became normal with respect to JNdi-1.

We explored the reasons for the appearance of $\mu^{142}\text{Nd}$ anomalies in the study of Upadhyay et al. (2009) by investigating the roles of fractionation correction method and choice of the terrestrial standard. Using various combinations of the most commonly employed methods, we observed that in a multi-dynamic mode of data acquisition, the *power-normalised exponential law* is the right method to correct for the mass fractionation. We also find that the suggested cause (by Roth et al., 2014b) for illusive appearance of negative $\mu^{142}\text{Nd}$ anomalies in Upadhyay et al. (2009)'s data, the time-gaps between the successive sequences in a multi-dynamic mode, had no role to play in the final corrected value of $^{142}\text{Nd}/^{144}\text{Nd}$. However, the terrestrial standard used by Upadhyay et al. (2009), i.e., LaJolla, with its higher $^{142}\text{Nd}/^{144}\text{Nd}$ than that of the currently prevalent JNdi-1, could have been the main cause for appearance of the negative anomalies. We, therefore, propose that all studies on early silicate Earth differentiation using ^{142}Nd as a tracer should use a single and homogeneous terrestrial standard, such as JNdi-1, to avoid issues with reproduction of anomalous compositions.

Supplementary data to this article can be found online at <http://dx.doi.org/10.1016/j.chemgeo.2017.06.036>.

Acknowledgements

We thank Anirban Chatterjee and Bivin Geo George for their help during the field trips. We greatly appreciate critical comments by R. Carlson on an earlier version of the manuscript. We sincerely thank Maud Boyet and an anonymous reviewer for their constructive comments and suggestions. This work was funded by the Department of Space, Government of India.

References

- Andreasen, R., Sharma, M., 2009. Fractionation and mixing in a thermal ionization mass spectrometer source: implications and limitations for high-precision Nd isotope analyses. *Int. J. Mass Spectrom.* 285, 49–57. <http://dx.doi.org/10.1016/j.ijms.2009.04.004>.
- Bennett, V.C., Brandon, A.D., Nutman, A.P., 2007. Coupled ^{142}Nd - ^{143}Nd isotopic evidence for Hadean mantle dynamics. *Science* 318, 1907–1910. <http://dx.doi.org/10.1126/science.1145928>.
- Boyet, M., Carlson, R.W., 2006. A new geochemical model for the Earth's mantle inferred from ^{146}Sm - ^{142}Nd systematics. *Earth Planet. Sci. Lett.* 250, 254–268. <http://dx.doi.org/10.1016/j.epsl.2006.07.046>.
- Boyet, M., Blichert-Toft, J., Rosing, M., Storey, M., Télouk, P., Albarède, F., 2003. ^{142}Nd evidence for early earth differentiation. *Earth Planet. Sci. Lett.* 214, 427–442. [http://dx.doi.org/10.1016/S0012-821X\(03\)00423-0](http://dx.doi.org/10.1016/S0012-821X(03)00423-0).
- Brandon, A.D., Lapen, T.J., Debaille, V., Beard, B.L., Rankenburg, K., Neal, C., 2009. Re-evaluating $^{142}\text{Nd}/^{144}\text{Nd}$ in lunar mare basalts with implications for the early evolution and bulk Sm/Nd of the moon. *Geochim. Cosmochim. Acta* 73, 6421–6445. <http://dx.doi.org/10.1016/j.gca.2009.07.015>.
- Caro, G., Bourdon, B., Birck, J., 2003. ^{146}Sm – ^{142}Nd evidence from Isua metamorphosed sediments for early differentiation of the Earth's mantle. *Nature* 423, 428–432. <http://dx.doi.org/10.1038/nature01639.1>.
- Caro, G., Bourdon, B., Birck, J.L., Moorbath, S., 2006. High-precision $^{142}\text{Nd}/^{144}\text{Nd}$ measurements in terrestrial rocks: constraints on the early differentiation of the earth's mantle. *Geochim. Cosmochim. Acta* 70, 164–191. <http://dx.doi.org/10.1016/j.gca.2005.08.015>.
- Habfast, K., 1998. Fractionation correction and multiple collectors in thermal ionization isotope ratio mass spectrometry. *Int. J. Mass Spectrom.* 176, 133–148. [http://dx.doi.org/10.1016/S1387-3806\(98\)14030-7](http://dx.doi.org/10.1016/S1387-3806(98)14030-7).
- Kinoshita, N., Paul, M., Collon, P., Deibel, M., DiGiovine, B., Greene, J.P., Henderson, D.J., Jiang, C.L., Marley, S.T., Nakanishi, T., Pardo, R.C., Rehm, K.E., Robertson, D., Scott, R., Schmitt, C., Tang, X.D., Vondrasek, R.Y.A., 2012. A Shorter ^{146}Sm half-life measured and implications for ^{146}Sm - ^{142}Nd chronology in the solar system. *Science* 80 (335), 1614–1617.
- Marks, N.E., Borg, L.E., Hutcheon, I.D., Jacobsen, B., Clayton, R.N., 2014. Samarium-neodymium chronology and rubidium-strontium systematics of an Allende calcium-aluminum-rich inclusion with implications for ^{146}Sm half-life. *Earth Planet. Sci. Lett.* 405, 15–24. <http://dx.doi.org/10.1016/j.epsl.2014.08.017>.
- O'Neil, J., Carlson, R.W., Francis, D., Stevenson, R.K., 2008. Neodymium-142 evidence for Hadean mafic crust. *Science* 321, 1828–1831. <http://dx.doi.org/10.1126/science.1161925>.
- Rizo, H., Boyet, M., Blichert-Toft, J., Rosing, M., 2011. Combined Nd and Hf isotope evidence for deep-seated source of Isua lavas. *Earth Planet. Sci. Lett.* 312, 267–279. <http://dx.doi.org/10.1016/j.epsl.2011.10.014>.
- Rizo, H., Boyet, M., Blichert-toft, J., Neil, J.O., Rosing, M.T., Paquette, J., 2012. The elusive Hadean enriched reservoir revealed by ^{142}Nd deficits in Isua Archean rocks. *Nature* 490, 96–100. <http://dx.doi.org/10.1038/nature11565>.
- Roth, A.S.G., Bourdon, B., Mojzsis, S.J., Touboul, M., Sprung, P., Guitreau, M., Blichert-Toft, J., 2013. Inherited ^{142}Nd anomalies in Eoarchean protoliths. *Earth Planet. Sci. Lett.* 361, 50–57. <http://dx.doi.org/10.1016/j.epsl.2012.11.023>.
- Roth, A.S.G., Bourdon, B., Mojzsis, S.J., Rudge, J.F., Guitreau, M., Blichert-Toft, J., 2014a. Combined ^{147}Sm - ^{143}Nd constraints on the longevity and residence time of early terrestrial crust. *Geochim. Geophys. Geosyst.* 15, 2329–2345. <http://dx.doi.org/10.1002/2014GC005313>. Received.
- Roth, A.S.G., Scherer, E.E., Maden, C., Mezger, K., Bourdon, B., 2014b. Revisiting the ^{142}Nd deficits in the 1.48 Ga Khariar alkaline rocks. *India. Chem. Geol.* 386, 238–248. <http://dx.doi.org/10.1016/j.chemgeo.2014.06.022>.
- Saji, N.S., Wielandt, D., Paton, C., Bizzarro, M., 2016. Ultra-high-precision Nd-isotope measurements of geological materials by MC-ICPMS. *J. Anal. At. Spectrom.* 31, 1490–1504. <http://dx.doi.org/10.1039/C6JA00064A>.
- Thirlwall, M.F., 1991. Long-term reproducibility of multicollector Sr and Nd isotope ratio analysis. *Chem. Geol.* 94, 85–104. [http://dx.doi.org/10.1016/0168-9622\(91\)90002-E](http://dx.doi.org/10.1016/0168-9622(91)90002-E).
- Upadhyay, D., Raith, M.M., Mezger, K., Bhattacharya, A., Kinny, P.D., 2006. Mesoproterozoic rifting and Pan-African continental collision in SE India: evidence from the Khariar alkaline complex. *Contrib. Mineral. Petrol.* 151, 434–456. <http://dx.doi.org/10.1007/s00410-006-0069-4>.
- Upadhyay, D., Scherer, E.E., Mezger, K., 2009. (^{142}Nd) evidence for an enriched Hadean reservoir in cratonic roots. *Nature* 459, 1118–1121. <http://dx.doi.org/10.1038/nature08089>.
- Wakaki, S., Tanaka, T., 2012. Stable isotope analysis of Nd by double spike thermal ionization mass spectrometry. *Int. J. Mass Spectrom.* 323–324, 45–54. <http://dx.doi.org/10.1016/j.ijms.2012.06.019>.